Punching shear strengthening of the flat slab using SIFCON

Wisam K. TUAMA ▪ Budapest University of Technology and Economics, Hungary
▪ awisamkamiltuamaalzweehm@edu.bme.hu
György L. BALÁZS ▪ Budapest University of Technology and Economics, Hungary
▪ balazs.gyorgy@emk.bme.hu
Érkezett: 2026. 01. 20. ▪ Received: 20. 01. 2026. ▪ https://doi.org/10.14382/epitoanyag-jsbcm.2025.16

Abstract

Punching shear failure in flat slabs remains one of the most critical issues in reinforced concrete structures due to its sudden and brittle nature. This research investigates the potential of using Slurry Infiltrated Fiber Concrete (SIFCON) as an alternative to traditional punching shear reinforcement in flat slabs cast from normal strength concrete (NSC). The fiber type was hooked-end steel fiber with a fraction volume of 6%. Five square flat slab specimens were cast; the first specimen was cast using NSC. Four of them were reinforced with maximum flexural steel to ensure failure by punching shear. In two of these slabs, SIFCON was used as a whole slab, but since it is expensive to use SIFCON for entire slabs, in others, SIFCON was used partially over an extended area in a form similar to a cross-shaped shear reinforcement and full or partial depth to improve the capacity to punching shear. The data demonstrate that SIFCON, when applied strategically, is a highly effective material for increasing punching shear capacity and improving post-punching behavior and ductility. Providing a realistic alternative to standard reinforcement approaches.
Keywords: flat slab, Slurry Infiltrated Fiber Concrete, punching shear, steel fibers, post-punching behavior
Kulcsszavak: síkfödém, cementhabarccsal injektált szálerősítésű beton (SIFCON), átszúródási nyírás

Wisam K. TUAMA
(1987), a Ph.D. student at the Department of Construction Materials and Technologies, Budapest University of Technology and Economics. Finished his Bachelor's (2010) in Civil Engineering at the College of Engineering, Thi Qar University in Iraq, and finished his master studies (2019) Master of Science in Construction Materials Engineering at the College of Engineering, Babylon University in Iraq. Research areas: Fiber Reinforced Concrete, durability of concrete, and Mechanical Properties of concrete. He is a member of the Hungarian Group of *fib*.

György L. BALÁZS
(1958), Civil Engineer, PhD, Dr. habil., Professor of structural engineering at the Department of Construction Materials and Technologies of Budapest University of Technology and Economics (BME). His main fields of activity are experimental investigation and modeling of RC, PC, FRC, FRP, HSC, HPC, LWC, fire resistance and fire design, durability, sustainability, bond, and cracking. He is chairman of several commissions and task groups of *fib*. He is the president of the Hungarian Group of Fib, Editor-in-Chief of the Journal "Concrete Structures". He was elected as President of *fib* for the period of 2011-2012. Since then, he has been Honorary President of *fib*. Chairman of *fib* Com 9 Dissemination of knowledge.

1. Introduction

Reinforced concrete flat slabs are increasingly favored in modern construction. By eliminating down-stand beams, the system relies on a simple, level formwork deck, streamlining site operations and accelerating the build. In multi-story projects, the reduced structural depth allows additional floors to be fitted within the same overall height. This efficiency cuts the quantity of façade materials, partition walls, and the length of mechanical, electrical, and plumbing runs, yielding notable savings in both resources and cost [1].

The main weakness of this type of roof is its failure with punching shear, as when making flat slabs using normal strength concrete (NSC), it is brittle and prone to punching shear failure, which occurs around columns at specific distances. Engineers have outlined several ways to raise the punching shear strength of flat slabs made with NSC. These include thickening the slab, adding column capitals, incorporating drop panels, placing additional shear reinforcement, and introducing advanced materials such as fiber-reinforced polymer (FRP) [2-4].

The cost and constructional intricacy of conventional strengthening techniques can, in many practical situations, offset the principal advantages of flat slab systems. Consequently, recent research has turned toward material solutions that increase punching shear capacity while preserving ease of execution. Other methods have been used to strengthen NSC flat slabs, using partially special types of concrete, some of which are high-strength concrete (HSC) or fiber-reinforced concrete (FRC). These concretes have been used by previous researchers in various ways and placed in different areas, depths, and shapes in flat slabs to perform their intended function. They have led to a noticeable improvement in the shear capacity of flat slabs [5-11]. In Slurry Infiltrated Fiber Concrete (SIFCON), the volume fraction of fibers is usually high, roughly 4% to 20% [12]. Ordinary FRC, by comparison, rarely exceeds about 2% fiber because it is mixed directly with cement, sand, and coarse aggregate, and workability quickly deteriorates [13]. SIFCON sidesteps this issue through a different production method: dense fibers are placed in the mold first, and a highly slurry mortar is then infiltrated to occupy the gaps between fibers. This manufacturing sequence yields a composite distinguished by exceptional toughness and markedly enhanced compressive, tensile, shear, and flexural strengths [14].

Published work on how best to employ SIFCON for upgrading reinforced concrete flat slabs is still sparse. In the present investigation, flat slab specimens were cast in which NSC was replaced, either wholly or partially, by SIFCON. Also, SIFCON was used partially over an extended area in a form similar to a cross-shaped shear reinforcement and full or partial depth to improve the resistance to punching shear. The study gauges how SIFCON replacement alters the slab's resistance to punching shear by comparing these configurations.

2. Experimental work

2.1 Materials and mix design

The materials composition adopted in this study, combining SIFCON and NCS, is detailed in *Table 1*. The binding materials comprise Portland cement type CEM I (42.5) along with silica fume. Normal quartz sand with a maximum particle size of

1 mm and 4 mm is used as a fine aggregate for SIFCON and NSC, respectively. 4/8 mm and 8/16 mm are used as coarse aggregates for NSC. *Fig. 1* shows the particle size distribution of aggregates. To ensure proper workability of the SIFCON mix, the high-range water-reducing admixture BASF Master Builders Solutions was incorporated. Flexural reinforcement was provided according to the specifications of ACI 318-19 [15], employing Ø10 mm deformed bars positioned on the tension side of the slabs to promote punching shear as the governing failure mode. In this investigation, steel fibers were hooked-end with a volume fraction of 6%. The type of fiber employed is illustrated in *Fig. 2*, while *Table 2* presents its technical characteristics as reported by the manufacturer.

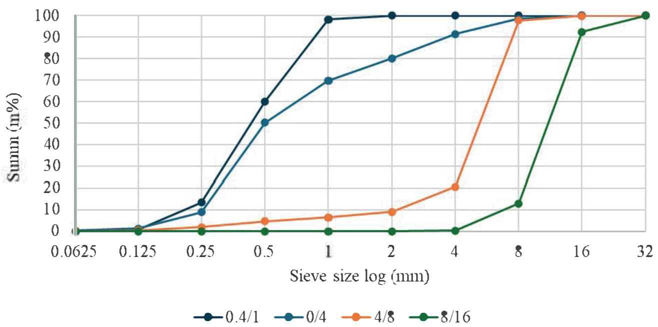

Fig. 1 Particle size distribution of aggregates
1. ábra Adalékanyagok szemmegoszlási görbéje

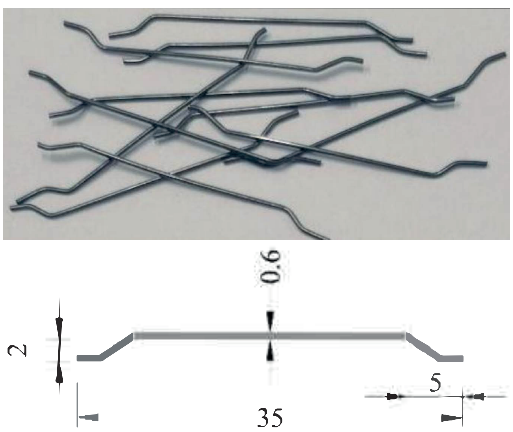

Fig. 2 Hooked-end steel fiber, the dimensions are in millimeters
2. ábra Visszahajlított végű acélszál, a méretek milliméterben értendők

Cement (kg/m³)	Sand (0.4-1) mm (kg/m³)	Sand (1-4) mm (kg/m³)	Coarse agg. (kg/m³)		Silica fume kg/m³ 10% rep.	Steel fiber %	w/b or w/c ratio	SP (by wt. of binder) %
			(4-8) mm	(8-16) mm				
370	–	924	462	462	–	–	50%	–
873	970	–	–	–	97	6	30%	1.75%

Table 1 NSC and SIFCON optimal mixing proportions for 1 m³
1. táblázat NSC és SIFCON optimális keverési arányai 1 m³-re vonatkoztatva

Fiber type	Length (mm)	Diameter (mm)	Density (kg/m³)	Tensile strength (MPa)
Hooked-end	35 ±5%	0.6 ±5%	7 850	1350

Table 2 Technical properties of the steel fibers
2. táblázat Az acélszálak műszaki jellemzői

A fiber volume content of 6% was selected in this study for the hooked-end fiber, as it was the most appropriate for the dimensions of the molds utilized. The mixing method adopted for the SIFCON mixture was developed based on previous studies and preliminary trials to ensure optimal workability. The mixing process involved initially blending the dry components for 3 minutes. Subsequently, two-thirds of the water, pre-mixed with the superplasticizer, was added and mixed for another 3 minutes. The remaining one-third of the water, also containing superplasticizer, was then introduced, and mixing continued for an additional 2 minutes.

2.2 Casting and testing samples and specimens

This investigation involved testing the compressive and flexural strengths of both NSC and SIFCON materials. Compressive strength was evaluated using cubes with dimensions of 150 mm for NSC and 100 mm for SIFCON. Flexural strength was assessed through prism specimens, sized 70×70×250 mm for NSC and 40×40×160 mm for SIFCON. For each test type and material, the reported values represent the results for 7 and 28 days.

The main objective of this study is to examine the structural behavior of flat slabs when using SIFCON in full or in part. The type of fibers used in SIFCON is hooked-end steel fiber. The experimental program consisted of testing 5 slab specimens; one reference specimen was cast with NSC. 2 NSC-SIFCON hybrid flat slab specimens with flexural reinforcement cast by using SIFCON partially over an extended area in a form similar to a cross-shaped shear reinforcement and full or partial depth. 2 SIFCON flat slab specimens cast by using SIFCON entirely with or without flexural reinforcement. In this study, square concrete slabs were utilized as test specimens, each measuring 600 mm on each side with a constant thickness of 60 mm. The specimens were classified according to the SIFCON concrete, the type of fibers used, or the depth of the SIFCON in composite slabs, as presented in *Table 3*. *Fig. 3* shows the overall slab geometries and reinforcement layout details.

Symbol	Details
N	Normal strength concrete (NSC) flat slab
S	Slurry infiltrated fiber concrete (SIFCON) flat slab without flexural reinforcement
S+R	Slurry infiltrated fiber concrete (SIFCON) flat slab with flexural reinforcement
N-S2+	NSC flat slab – the SIFCON in a cross-shaped form with 20 mm depth in the tension side
N-S6+	NSC flat slab – the SIFCON in a cross-shaped form with full flat slab depth

Table 3 The symbols of the slab and their meanings.
3. táblázat A födémek jelölései és jelentésük

Prior to the casting process, all constituent materials were carefully prepared and proportioned according to the mix volume. The flat slab specimens, each measuring 600×600×60 mm, were formed using wooden molds supported by external iron frames and placed on a steel base to ensure dimensional stability throughout the casting. Before each casting, molds were thoroughly cleaned, coated with release agent, and leveled on a flat surface.

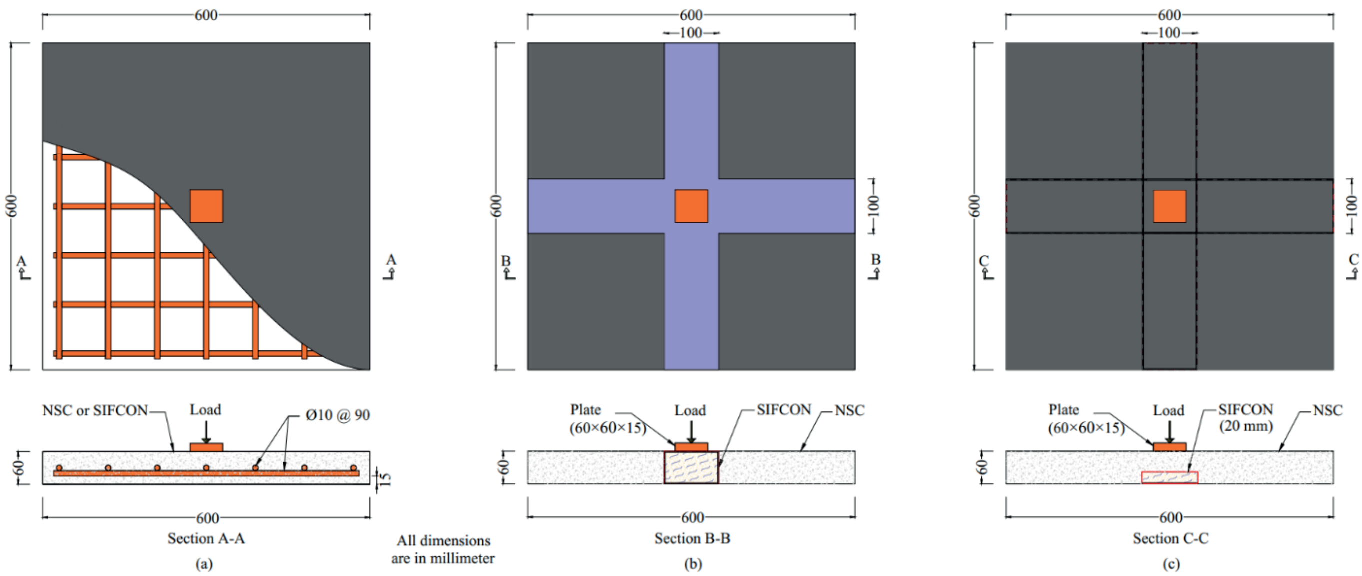

Fig. 3 Specimen dimensions and layout: (a) NSC or SIFCON flat slab with reinforcement details; (b) Hybrid flat slab with full depth of SIFCON; (c) Hybrid flat slab with partial depth of SIFCON

3. ábra A próbatestek méretei és elrendezése: (a) NSC vagy SIFCON síkfödém vasalási részletekkel; (b) Hibrid síkfödém teljes vastagságú SIFCON réteggel; (c) Hibrid síkfödém részleges vastagságú SIFCON réteggel

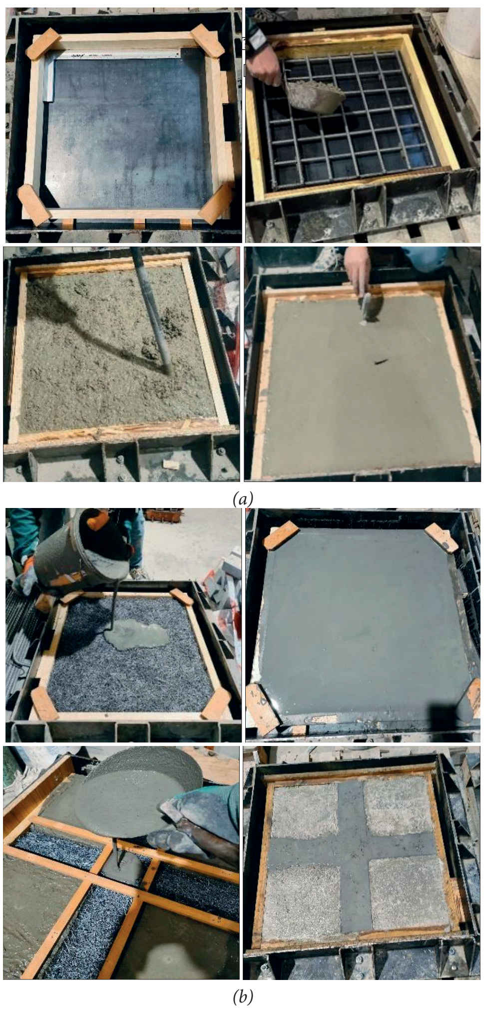

Fig. 4 The steps of casting the different types of flat slab concrete (a- NSC flat slab, b- SIFCON slab and NSC-SIFCON flat slabs).

4. ábra A különböző típusú síkfödém betonok betonozási lépései (a- NSC síkfödém, b- SIFCON födém és NSC-SIFCON síkfödémek)

The sequence of casting for various concrete types is illustrated in *Fig. 4*. For slabs made with NSC, reinforcement meshes were accurately placed inside the molds, ensuring proper bottom cover. In SIFCON slabs, the steel fibers were introduced in a single batch into the mold before the slurry was poured, allowing the mix to penetrate and encapsulate the fibers.

In the case of hybrid flat slabs, a fine galvanized steel mesh was positioned precisely at the interface between the NSC and SIFCON regions. This mesh was anchored to the bottom reinforcement and held in position from above using a wooden formwork system to control the geometry, as shown in *Fig. 5b*.

Upon completion of the 28-day curing period, structural load tests were performed on all slab specimens under monotonically increasing central loading until ultimate failure was reached. The loading way utilized a precision-calibrated electro-hydraulic testing machine with a rated capacity of 600 kN, as depicted in *Fig. 5*. The load application was controlled to ensure uniform rate progression and avoid dynamic effects. Each slab was simply supported along all four sides over an effective span of 500 mm using a custom-fabricated steel frame integrated within the testing setup. Loading was applied using a 60×60 mm steel stub column. All tests were conducted under a controlled displacement rate of 0.5 mm/min. To monitor deflection behavior, linear variable differential transducers (LVDTs) were positioned at the slab center and two quarter-span points on opposite sides of the applied load. Key response parameters recorded included the cracking load, the ultimate load associated with punching shear or flexural failure, mid-span deflection, and the averaged deflections at the quarter-span points.

The ultimate deflection was defined following Kaka et al. [16] as the deflection corresponding to a post-peak load reduction to 80% of the maximum load. Given the emphasis on the high ductility behavior of SIFCON in this investigation, particular attention was directed to the structural response beyond the peak load. Two critical deflection points in the post-peak stages were identified: one at 80% and the second at 60% of the peak load. These deflection values are referred to herein as u_1 and u_2, respectively, and were used to assess the residual load-carrying capacity and the contribution of fibers under advanced deformation.

3. Results and discussion

3.1 Mechanical properties

In this work, the flexural and compressive strengths of SIFCON and NSC concrete are tested. The cubes and prisms made for this purpose were evaluated for compressive and flexural strength at 7 and 28 days. The NSC and SIFCON are displayed in *Table 4*. The findings demonstrate that SIFCON with hooked-end steel fiber has a substantially higher compressive and flexural tensile strength than NSC. The capacity of fibers to limit and stop fracture development, as well as to reduce the rate and direction of crack propagation, can be explained by their increased strength. *Table 4* also shows the increases in both compressive and flexural strength for SIFCON relative to the reference NSC at 28 days.

Fig. 5 Punching shear test of flat slabs
5. ábra Síkfödémek átszúródási nyíróvizsgálata

Type of concrete	Compressive strength (MPa)		The standard deviation	Flexural strength (MPa)		The standard deviation	The percentage increase (%) in 28 days compared to NSC	
	7 days	28 days		7 days	28 days		Compressive strength	Flexural strength
NSC	31	43	1.4	3.7	4.8	0.4	–	–
SIFCON	89	118	3.08	23.5	32	2.2	174	567

Table 4 The mechanical properties results of the NSC and SIFCON
4. táblázat Az NSC és a SIFCON mechanikai tulajdonságainak eredményei

3.2 First crack strength

The first crack loads, for the various slabs, are summarized in *Table 5*. Also, the same table shows the deflection of the center and the average deflection of two quarters at the first crack. The results show that using SIFCON increased the first crack strength of the slab. The first crack strength increased for hybrid slabs by 56% for the slab in which the SIFCON was used in the form of a cross-shaped with full depth. The highest percentage increase in first crack was reached in the slab made entirely of SIFCON using hooked-end steel fibers. The percentage in the S+R slab reached 342%.

The main reason behind SIFCON's remarkable ability to withstand first cracking loads is its dense fiber, which comprises 6% of the slab's volume. The closely spaced steel fibers intersect at every potential crack plane, so once a microscopic crack forms, the fibers bridge it, absorbing tensile forces and distributing stress over a much larger area. This bonding keeps crack widths microscopic, meaning the element must be subjected to significantly greater external loads before any visible cracking becomes apparent.

Specimen	P_{cr} (kN)	Δ_c (mm)	Δ_q (mm)	η_f (%)
N	11.18	1.23	0.21	–
S	42.72	2.61	2.35	282
S+R	49.43	2.95	2.69	342
N-S2+	16.92	1.83	1.20	51
N-S6+	17.43	1.91	1.24	56

Note: P_{cr} = First cracking load; η_f = The percentage of improved first crack strength compared to specimen N; Δ_{cf} = Center deflection at first cracking load; Δ_{qf} = Quarters av. deflection at first cracking load.

Table 5 The first crack load and deflection of the specimens at the first cracks
5. táblázat Az első repedéshez tartozó teher és lehajlás a próbatesteknél

3.3 Failure mode and crack pattern

Fig. 6 maps the cracking patterns that developed on the tension face of every slab. Three discrete failure mechanisms were identified: punching shear, flexure, and a coupled punching shear-flexural mode. The reference specimen N failed in punching shear: radial cracks nucleated directly beneath the load and spread outward to form a circumferential ring, accompanied by local concrete spalling. A purely flexural response characterized S and N-S2+ specimens, where cracks originated at mid-span and propagated diagonally toward the supports. Specimens S+R and N-ST6+ exhibited the mixed mode: load-induced longitudinal cracks first appeared parallel to the reinforcement, then evolved into diagonal and peripheral circular cracks. In hybrid slabs, the initial crack consistently formed along the interface between the SIFCON layer and the surrounding NSC, and continued outward until the peak load, when the punching shear cone was fully established.

Deflection records underscore the ductility advantages conferred by SIFCON. The reference N slab displayed virtually no post-peak deformation, 4.82 mm at peak load and 5.33 mm at the u_2 stage, revealing a brittle response. In contrast, SIFCON and hybrid flat slabs showed substantial displacement capacity beyond first cracking. The most pronounced increase occurred in the S+R specimen, whose deflection rose from 12.6 mm at peak load to 24.8 mm at u_2. This post-peak ductility grew with the SIFCON volume fraction. Moreover, hooked-end steel fibers improved energy absorption and postponed failure, reaffirming that a higher fiber dosage markedly enhances both ductility and load-carrying capacity in the later stages of loading.

3.4 Peak load and load-deflection response

Table 6 compiles the maximum (peak) loads, the corresponding mid-span deflections, and the average deflection of two quarters at the peak load, together with the percentage increase in peak load relative to the reference slab N. *Fig. 7* charts the complete load-deflection curve for each specimen. The data confirm that enlarging the SIFCON portion of a slab generally raises its punching shear capacity.

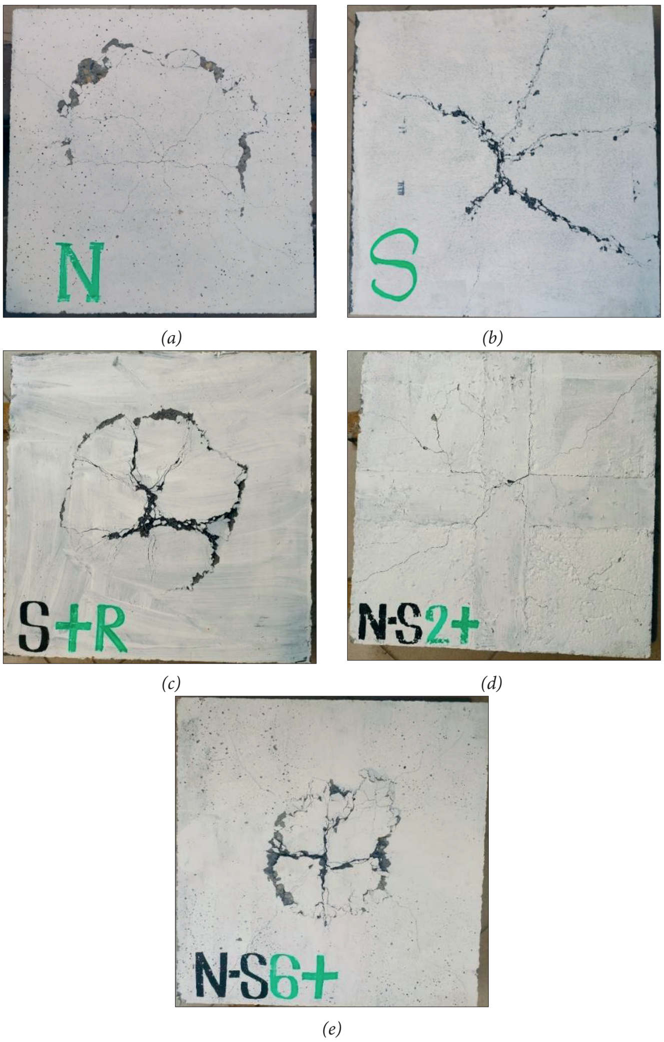

Fig. 6 Crack pattern on the tension face of flat slab specimens: (a) N ; (b) S; (c) S+R; (d) N-S2+; (e) N-S6+
6. ábra Repedéskép a síkfödém próbatestek húzott oldalán: (a) N; (b) S; (c) S+R; (d) N-S2+; (e) N-S6+

The greatest strength enhancements were obtained for slab S+R, whose peak loads were 118% higher than those of the N flat slab. Among the hybrid cross-shaped specimens, the best performance was achieved by N-S6+ flat slab, which exceeded the reference slab's peak load by roughly 36%. Also, the presence of SIFCON altered the failure mode from brittle to a more ductile flexural response. For hybrid slabs, the gap between u_1 and u_2 widened as the thickness of the SIFCON layer was increased. In slabs cast entirely with SIFCON, this deflection gap was larger in the S+R slab, further promoting a switch from punching to flexural failure and greatly enhancing ductility, as observed in S and S+R specimens.

Overall, the study demonstrates that even a modest amount of SIFCON, applied as a cross-shaped throughout the thickness, can deliver substantial strength gains while providing excellent ductility. The difference between the deflection at peak load and the u_2 stage reached roughly 12 mm in N-S6+ slab cases. These findings emphasize the promise of SIFCON for flat slab construction: significant improvements in capacity and toughness can be achieved without increasing slab thickness, adding drop panels, or column capitals.

Specimen	P_p (kN)	Δ_{cp} (mm)	Δ_{qp} (mm)	η_p (%)
N	50.18	4.82	2.25	–
S	93.14	7.74	4.25	86
S+R	109.3	5.25	8.41	118
N-S2+	56.01	8.41	3.21	12
N-S6+	68.05	11.46	3.32	36

Note: P_p = Peak load by (kN); Δ_{cp} and Δ_{qp} = Center and Quarters av. deflection by (mm) at peak load, respectively; η_p = The percentage of improved peak load compared to specimen N.

Table 6 The peak load and deflection of the specimens at the peak load
6. táblázat A maximális teher és a hozzá tartozó lehajlás a próbatesteknél

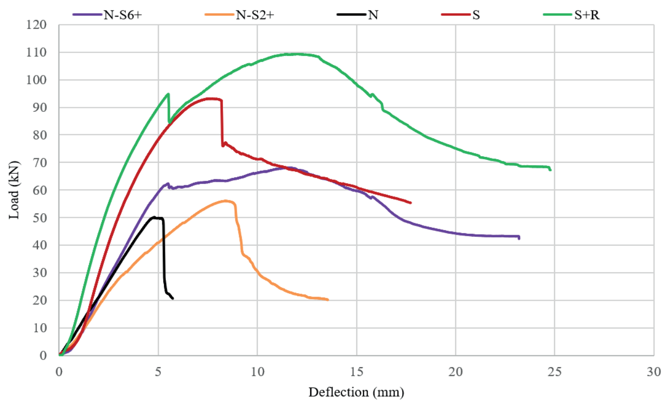

Fig. 7 The load-center deflection curves of all specimens
7. ábra Az összes próbatest teher-középponti lehajlás görbéje

3.5 Ductility

Ductility, μ, describes the capacity of a structural member to undergo substantial deformation after yield. In this study, it is expressed as the ratio of the ultimate displacement, Δ_u, to the corresponding yield displacement, Δ_y, by *Eq. (1)* and the procedure proposed by Lim and Hong [17]. The ultimate displacement is taken as the deflection recorded when the applied load has fallen to 80% of the specimen's peak value. The secant stiffness at a point two-thirds of the measured peak load is used to idealize the elastoplastic curve that passes through the peak point of the load-deflection curve, and the displacement at an intersecting point between the two lines is used to determine the yield point on the curve [17-19].

Because the slabs exhibited continuing deformation after peak load, ductility ratios were evaluated at two ultimate stages, u_1 and u_2, to capture the influence of fiber reinforcement on post-peak behavior. The resulting indices, μ_1 and μ_2, are reported in *Table 7* and provide a clearer picture of how fiber type and distribution affect the later stages of the response.

$$\mu = \frac{\Delta u}{\Delta y} \qquad \text{eq. (1)}$$

Specimen	P_y (kN)	Δ_{cy} (mm)	Δ_{cu1} (mm)	Δ_{cu2} (mm)	$\mu 1$	$\mu 2$	$\eta_{\mu 1}$ (%)	$\eta_{\mu 2}$ (%)
N	48.90	4.65	5.22	5.30	1.12	1.14	–	–
S	83.44	5.56	8.85	17.54	1.59	3.15	42	176
S+R	93.94	5.40	16.71	24.78	3.09	4.59	176	303
N-S2+	49.99	6.67	9.1	9.72	1.36	1.46	21	28
N-S6+	61.00	5.68	16.36	23.51	2.88	4.14	157	263

Note: P_y = yield load by (kN); Δ_{cy}= Center deflection by (mm) at yield load; $\Delta_{c(u1\ and\ u2)}$ = Center ultimate deflection by (mm) u_1 and u_2 respectively; μ_1 and μ_2 = the ductility 1 and 2; $\eta_{\mu 1}$ and $\eta_{\mu 2}$ = The percentage of improved ductility 1 and 2 compared to specimen N.

Table 7 The ductility results

7. táblázat Duktilitási eredmények

Table 7 demonstrates that embedding SIFCON in the slab markedly elevates its ductility. During the stage u_1, ductility increases steadily, while a far more pronounced gain emerges in the second stage u_2. For hybrid flat slabs, most clearly in specimen N-S6+, where a cross-shaped SIFCON extends through the full thickness, the greatest benefit appears in the transition between these two stages. After the longitudinal reinforcement fully yields, the SIFCON fibers engage, bridging and confining cracks so effectively that the slab sustains its load-bearing capacity for an extended period, and the failure mode shifts from brittle to ductile. These results confirm the study's key premise: outstanding ductility can be achieved with only a modest volume of SIFCON.

3.6 Inclination of cracks and rotation of slabs

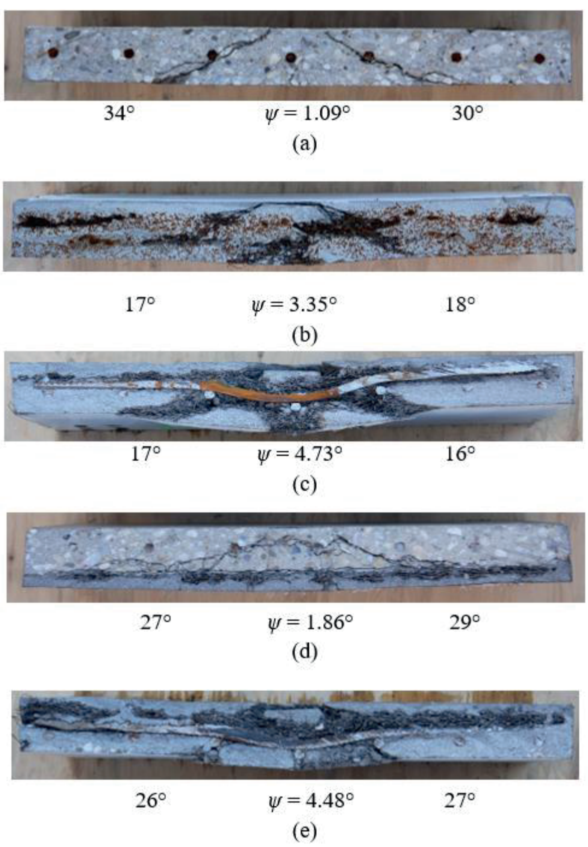

Fig. 8 Inclination of cracks and rotation of flat slab specimens: (a) N; (b) S; (c) S+R; (d) N-S2+; (e) N-S6+

8. ábra A repedések dőlésszöge és a síkfödém próbatestek elfordulása: (a) N; (b) S; (c) S+R; (d) N-S2+; (e) N-S6+

After completing the slab tests, the rotation of each slab about the loading zone was recorded, and the specimens were subsequently sectioned longitudinally to delineate the dominant crack patterns *Fig. 8*. By mapping cracks on both the top and bottom faces, the punching shear cone angle, defined as the inclination between the failure surface and the vertical plane, was established. Results show that this angle on the tensile face decreases monotonically with higher SIFCON content. This finding demonstrates that the critical cracks migrate progressively away from the critical punching shear area, transforming the failure mode from brittle to ductile. Moreover, the slab's rotation angle increases with SIFCON incorporation, particularly when larger SIFCON regions are provided.

4. Conclusion

This study evaluates the structural performance of flat slabs strengthened either fully with SIFCON or partially through a hybrid system combining SIFCON with NSC. The experimental program measured the compressive and flexural strengths of both SIFCON and NSC, determined punching shear load, deflection, ductility, and rotation, and recorded crack patterns together with crack inclinations. The results highlight the efficiency of adding SIFCON in boosting punching shear capacity and improving the behavior of flat slabs. The study presents a series of conclusions:

1. At 28 days, SIFCON had greater compressive and flexural strengths of 118 and 32 MPa, respectively. Comparing SIFCON to the reference NSC, the percentage increase in compressive and flexural strength of SIFCON was 174% and 567% respectively.
2. The slabs made entirely of SIFCON demonstrated a substantial improvement in the first cracking load. With a 342% improvement above the reference N flat slab, and in hybrid flat slabs, the increase in first cracking load was 56%.
3. When compared to the N flat slab, the maximum load capacity of the SIFCON flat slab shows a significant improvement. The higher percentage increase for SIFCON flat slabs compared to the reference N flat slab was 118% for the S+R specimen, and for the hybrid flat slabs, it was 36% for the N-S6+ specimen.
4. The load-deflection curves showed that all the slabs that used SIFCON entirely or partially had a high ductility and gradual post-peak decline, unlike the N flat slab, which failed suddenly. The percentage increase in ductility $\eta_{\mu 2}$ was 303% in the S+R slab and 263% in the N-S6+ slab at the u_2 stage compared to the reference N flat slab.
5. The average inclination angle of the punching shear cone cracks of the N flat slab is about 32°. On the other hand, the SIFCON slabs record 17°, demonstrating the material's exceptional capacity to prevent cracks. The smallest angle of the hybrid flat slabs was 26° for the N-S6+ specimen. The rotation of the S+R flat slab around the load point reaches roughly 4.7°.

5. Acknowledgement

The authors would like to express their sincere gratitude to Betonmix Ltd. for generously providing the steel fibers used in this study. Their valuable support and contribution significantly contributed to the successful completion of the experimental work.

References

[1] Weerasinghe P., Nguyen K., Mendis P., Guerrieri M., "Large-scale experiment on the behavior of concrete flat slabs subjected to standard fire", J Build Eng 30 (2020) 101255. https://doi.org/10.1016/j.jobe.2020.101255

[2] Tahmoorian, F., Nemati, S., Sharafi, P., Samali, B., & Khakpour, S. (2021). Punching behavior of foam-filled modular sandwich panels with high-density polyethylene skins". Journal of Building Engineering, 33, 101634. https://doi.org/10.1016/j.jobe.2020.101634

[3] Saleh, H., Kalfat, R., Abdouka, K., & Al-Mahaidi, R. (2019). "Punching shear strengthening of RC slabs using L-CFRP laminates". Engineering Structures, 194, 274–289. https://doi.org/10.1016/j.engstruct.2019.05.050

[4] Halvoník, J., Kalická, J., Majtánová, L., & Minárová, M. (2019). "Reliability of models aimed at evaluating the punching resistance of flat slabs without transverse reinforcement". Engineering Structures, 188, 627–636. https://doi.org/10.1016/j.engstruct.2019.03.055

[5] Nguyen, L., Rovn, M., Tran, T., & Nguyen, K. (2011). "Punching shear resistance of steel fiber reinforced concrete flat slabs". Procedia Engineering, 14, 1830–1837. https://doi.org/10.1016/j.proeng.2011.07.230

[6] Facconi, L., Minelli, F., & Plizzari, G. (2016). "Steel fiber reinforced self-compacting concrete thin slabs: Experimental study and verification against Model Code 2010 provisions". Engineering Structures, 122, 226–237. https://doi.org/10.1016/j.engstruct.2016.04.030

[7] Qi, J., Cheng, Z., Zhou, K., Zhu, Y., Wang, J., & Bao, Y. (2021). Experimental and theoretical investigations of UHPC-NC composite slabs subjected to punching shear-flexural failure. Journal of Building Engineering, 44, 102662. https://doi.org/10.1016/j.jobe.2021.102662

[8] Brisid, I., Joao, P., Carla, M., & Antonio, P. (2022). "Behavior of flat slabs with partial use of high-performance fiber reinforced concrete under monotonic vertical loading". Engineering Structures, 264, 114471. https://doi.org/10.1016/j.engstruct.2022.114471

[9] Yehia, E., Khalil, A. H., Mostafa, E. E., & El-Nazzer, M. A. (2023). "Experimental and numerical investigation on punching behavior of ultra-high performance concrete flat slabs". Ain Shams Engineering Journal, 14, (10), 102208. https://doi.org/10.1016/j.asej.2023.102208

[10] Tuama, W. K., Balázs, G. L. "Behavior of Flat Slabs with Partial Use of SIFCON Subjected to Concentrated Loading", Periodica Polytechnica Civil Engineering, 69(4), pp. 1333–1344, 2025. https://doi.org/10.3311/PPci.41452

[11] Zamri N. F., Mohamed R. N., Awalluddin D., and Abdullah R., "Experimental evaluation on punching shear resistance of steel fiber reinforced self-compacting concrete flat slabs," Journal of Building Engineering, vol. 52, Art. no. 104441, 2022. https://doi: 10.1016/j.jobe.2022.104441

[12] Tauma, W. K., and Balázs, G. L, (2024). "Properties of fibers and mortar of slurry infiltrated fiber concrete (SIFCON)." 14th Central European Congress on Concrete Engineering. ISPN 978-80 908943-1-0, 454–465.

[13] ACI Committee 544. (2002). "State-of-the-Art report on fiber reinforced concrete (ACI 544.1R-96). American Concrete Institute.

[14] Tauma, W. K., and Balázs, G. L, (2023). "Impact and blast resistance of slurry infiltrated fiber concrete (SIFCON): a comprehensive review". Concrete Structures Journal, 24, 129-136. https://doi.org/10.32970/CS.2023.1.18

[15] ACI Committee 318. (2019). "Building code requirements for structural concrete (ACI 318-19) ". American Concrete Institute.

[16] Chao S.-H., Kaka V., Kim J., (2016) Formulating Constitutive Stress-Strain Relations for Flexural Design of Ultra High-Performance Fiber-Reinforced Concrete, in: International Interactive Symposium on Ultra-High Performance Concrete, Iowa State University Digital Press.

[17] Lim W., Hong S., Shear Tests for Ultra-High Performance Fiber Reinforced Concrete (UHPFRC) Beams with Shear Reinforcement, International Journal of Concrete Structures and Materials 10 (2016) 177–188. https://doi.org/10.1007/s40069-016-0145-8.

[18] Européen C., Eurocode 2: Design of concrete structures-Part 1-1: General rules and rules for buildings, London: British Standard Institution (2004) 37.

[19] Sukontasukkul P., Nimityongskul P., Mindess S., Effect of loading rate on damage of concrete, Cement and Concrete Research 34 (2004) 2127–2134. https://doi.org/https://doi.org/10.1016/j.cemconres.2004.03.022.

Ref.:
Tuama, Wisam K. – **Balázs**, György L.: *Punching shear strengthening of the flat slab using SIFCON*
Építőanyag – Journal of Silicate Based and Composite Materials, Vol. 77, No. 4 (2025), 124–130 p.
https://doi.org/10.14382/epitoanyag-jsbcm.2025.16